Intra- and Intermolecular Photoinduced Energy and Electron Transfer between Oligothienylenevinylenes and *N*-Methylfulleropyrrolidine

Joke J. Apperloo,[†] Corinne Martineau,[‡] Paul A. van Hal,[†] Jean Roncali,*[,‡] and René A. J. Janssen*[,†]

Laboratory for Macromolecular and Organic Chemistry, Eindhoven University of Technology, P.O. Box 513, 5600 MB Eindhoven, The Netherlands, and Ingénierie Moléculaire et Matériaux Organiques, CNRS UMR 6501, Université d'Angers, 2 Boulevard Lavoisier, F-49045 Angers Cedex, France

Received: July 31, 2001; In Final Form: October 3, 2001

The photophysical properties of a homologous series of oligothienylenevinylenes (*n*TVs) and the inter- and intramolecular photoinduced energy- and electron-transfer processes between an *n*TV as a donor and *N*-methylfulleropyrrolidine (MP−C_{60}) as an acceptor are described as a function of oligomer length ($n = 2$, 3, 4, 6, 8, and 12) in apolar and polar solvents. Whereas the shorter oligomers fluoresce and have singlet excited-state [*n*TV(S_1)] lifetimes of 280 ps (2TV) and 1360 ps (3TV), the S_1 lifetimes of the longer oligomers ($n > 3$) are extremely short because of a fast thermal decay, resulting in negligible quantum yields for fluorescence and intersystem crossing to the triplet state [*n*TV(T_1)]. Using photoinduced absorption (PIA) spectroscopy, we demonstrate, however, that the *n*TV(T_1) state can be populated indirectly via intermolecular triplet energy transfer using photoexcited MP−C_{60} as a triplet sensitizer for $n > 2$. This enabled the spectral determination of the *n*TV ($T_n \leftarrow T_1$) transition as a function of chain length ($n = 3-12$) in toluene ($\epsilon = 2.38$). In a more polar solvent, *o*-dichlorobenzene (ODCB, $\epsilon = 9.93$), the MP−C_{60}(T_1) state acts both as an oxidizing agent toward the *n*TVs, resulting in the formation of a metastable radical ion pair (*n*$TV^{+\bullet}$ + MP−$C_{60}^{-\bullet}$) for $n > 2$, and as a triplet sensitizer, to produce the *n*TV(T_1) state. In addition to the intermolecular transfer reactions, we investigated the corresponding *intra*molecular photoinduced energy- and electron-transfer reactions in systems in which MP−C_{60} and *n*TV ($n = 2-4$) are covalently linked. The results indicate that, after photoexcitation of the *n*TV moiety, an ultrafast singlet energy transfer to MP−C_{60} occurs, followed by an *intra*molecular electron transfer. The *intra*molecularly charge-separated state is the lowest-energy excited state in polar media, e.g., ODCB. In apolar media, e.g., toluene, the formation of the *intra*molecularly charge-separated state occurs only for $n > 2$ and concurrent with fluorescence and intersystem crossing to the MP−C_{60}(T_1) state. The discrimination between energy and electron transfer is rationalized using a continuum model.

1. Introduction

Composite films of conjugated polymers (electron donors) and [60]fullerene derivatives (electron acceptors) have been successfully used as the active layer in photovoltaic devices.[1−6] An ultrafast (subpicosecond) forward electron-transfer reaction causes the quantum efficiency of the charge separation process to be close to unity.[7−9] Moreover, the recombination of positive and negative charges is comparatively slow and extends into the millisecond range,[10] which makes the collection of photoinduced charges feasible. In addition to an ultrafast direct electron transfer, recent studies on covalently bonded donor−C_{60} systems provide examples of very fast singlet energy transfer ($k_{ET} > 10^{12}$ s^{-1}) from the photoexcited π-conjugated donor moiety to the C_{60} acceptor moiety, preceding the formation of a charge-separated state.[11−20]

One important factor governing charge separation is the oxidation potential of the π-conjugated donor, which should be low in order to stabilize the charge-separated state. In that regard, it is surprising that poly(thienylenevinylene) (PTV) previously received no attention for use in photovoltaic devices. Both PTV and well-defined oligothienylenevinylenes (*n*TV, with *n* being the number of thiophene units) are known to exhibit lower oxidation potentials and smaller band gaps in comparison to, for example, oligothiophenes (*n*Ts) and oligo(*p*-phenylenevinylene)s (*n*PVs) with comparable chain lengths.[21] The *n*TV absorption energies and redox potentials show linear relationships to the reciprocal chain length ($1/N$, with N being the number of double bonds),[21] with a noticeably steep gradient. A deviation from linearity, suggesting a convergence limit, is only reached at high chain lengths (16TV, $N = 47$), significantly higher than for the corresponding *n*Ts and *n*PVs.[22] These features indicate that large effective conjugation lengths and correspondingly low band gaps can be reached. This is confirmed by recent calculations showing that *n*TV oligomers exhibit extensive π-electron delocalization along the molecular backbone.[23]

Although these reduced band gaps can be expected to improve the collection efficiency of photovoltaic devices through better overlap of the absorption spectrum of the active layer with solar emission, the photophysical properties of thienylenevinylene oligomers and their use as electron donors toward C_{60} have not been described in detail.

Another important consideration concerning the formation of a charge-separated state is the Coulomb screening of photo-

* Corresponding authors. E-mail: jean.roncali@univ-angers.fr. E-mail: r.a.j.janssen@tue.nl.
[†] Eindhoven University of Technology.
[‡] Université d'Angers.

10.1021/jp012936f CCC: $22.00
Published on Web 12/08/2001

CHART 1

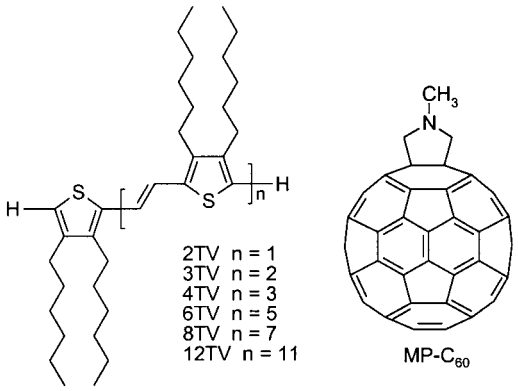

generated charges via the relative permittivity of the medium. In more polar solvents, a charge-separated state will be stabilized as a result of the solvation of the formed radical ions. Consequently, valuable information on the fundamental energetic and kinetic factors that govern photoinduced *inter*molecular electron transfer in *n*TV donors and [60]fullerene acceptors can be obtained by studying a homologous series of well-defined *n*TVs in solvents with different polarities. Insight into the photophysics of the corresponding *intra*molecular electron- and energy-transfer processes can be obtained when the donor and acceptor molecules are connected via a covalent bond, and a number of C_{60}-based molecular dyads and triads have been constructed in recent years for this purpose.[24−28]

Here, we explore *inter*molecular photoinduced energy and electron transfer as functions of chain length in solutions containing *n*TV ($n = 2$, 3, 4, 6, 8, and 12) and *N*-methylfulleropyrrolidine (MP−C_{60}) (Chart 1). Because fluorescence and intersystem crossing from the lowest-energy singlet excited state in *n*TVs is found to be negligible for $n > 3$, the *n*TV triplet state [*n*TV(T_1)] state cannot be populated via direct photoexcitation. We demonstrate that, by using the MP−C_{60}(T_1) state as a sensitizer, it is possible to generate the *n*TV(T_1) state in apolar media and a metastable $nTV^{+\bullet}$ + MP−$C_{60}^{-\bullet}$ radical ion pair in polar media via *inter*molecular energy and electron transfer, respectively. The solvent-dependent discrimination between photoinduced energy- and electron-transfer processes is rationalized on the basis of a quantitative model that describes the screening of charges as a function of the polarity of the solvent.

Purely *intra*molecular photoinduced processes have been analyzed in dyads and triads, in which the *n*TV chain ($n = 2-4$) is covalently bonded to one or two MP−C_{60} moieties (Chart 2). In these systems, an ultrafast *n*TV(S_1) → MP−C_{60}(S_1) *intra*molecular singlet energy transfer precedes *intra*molecular electron transfer. The latter process competes with fluorescence from MP−C_{60}(S_1) and intersystem crossing to MP−C_{60}(T_1) and is more favored in polar solvents.

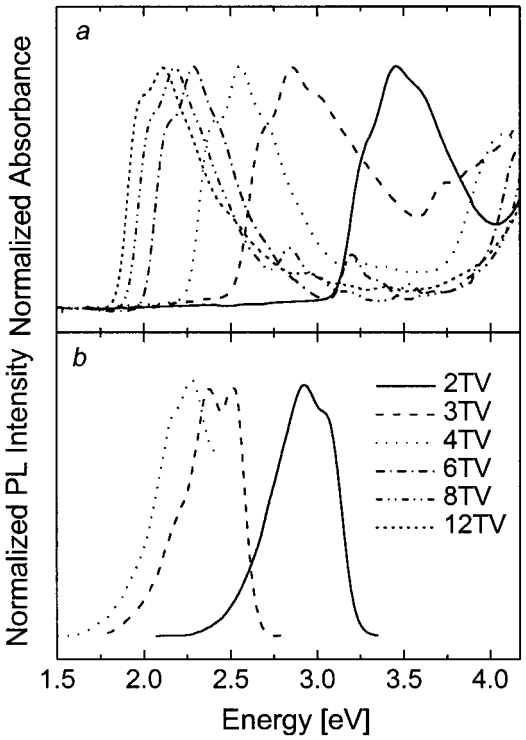

Figure 1. (a) Normalized absorption spectra of 2−12TV in 2-MeTHF at 295 K. (b) Normalized emission spectra of 2TV, 3TV, and 4TV in toluene. The absorption and emission characteristics are similar in both solvents, apart from a small red shift of about 0.02 eV in toluene compared to 2-MeTHF.

2. Results and Discussion

2.1. Absorption, Fluorescence, and Photoinduced Absorption Spectroscopy of *n*TVs in Solution. Figure 1a shows that the $\pi-\pi^*$ absorption spectra of the *n*TV oligomers in solution shift to lower energies with longer chain lengths as a result of the increased effective conjugation lengths. The shorter *n*TV oligomers (2TV, 3TV, and 4TV) fluoresce, but with moderate to very low quantum yields (Table 1). The normalized fluores-

CHART 2

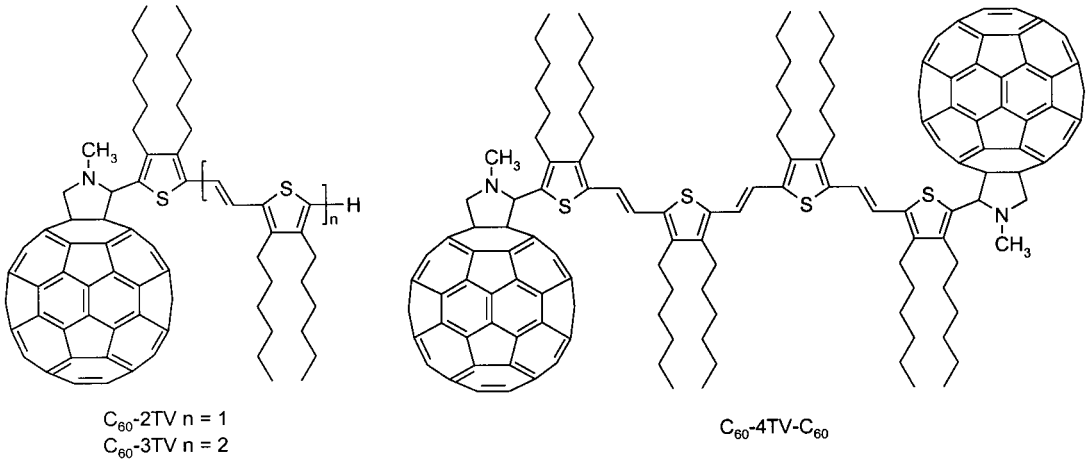

TABLE 1: Fluorescence Quantum Yield [ϕ_{PL}(*n*TV)], Lifetime of the Singlet Excited State [τ(*n*TV)], and Rate Constants for Radiative Decay (k_R) and Nonradiative Decay (k_{NR}) for *n*TVs as Determined by Experiment and the Strickler−Berg Relation

	experiment			Strickler−Berg		
	ϕ_{PL}(*n*TV)[a]	τ(*n*TV)[b] (ps)	k_R[c] (s^{-1})	k_R[d] (s^{-1})	k_{NR}[e] (s^{-1})	τ(*n*TV)[f] (ps)
2TV	0.057	280	2.0×10^8	3.4×10^8	5.6×10^9	170
3TV	0.027	1360	0.2×10^8	3.7×10^8	1.3×10^{10}	73
4TV	0.0009			3.5×10^8	3.8×10^{11}	2

[a] Determined using anthracene (in ethanol) and quininesulfatedihydrate (in 1 N H_2SO_4) as a reference.[46] [b] Determined by TCSPC. [c] $k_R = \phi_{PL}/\tau$. [d] Determined with the Strickler−Berg formula (eq 1).[31] [e] Determined using eq 2 and the experimental value of ϕ_{PL}(*n*TV). [f] Determined using eq 3 and the experimental value of ϕ_{PL}(*n*TV).

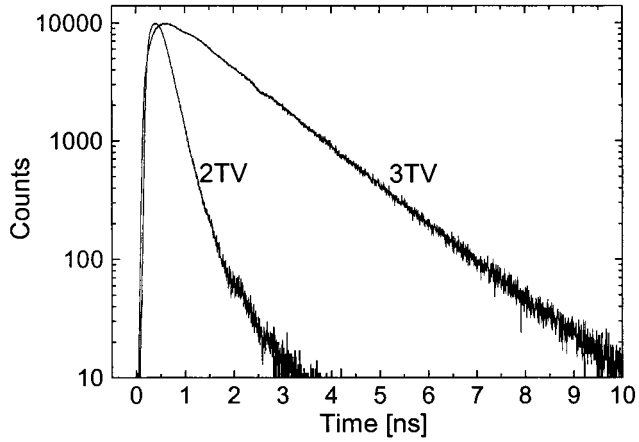

Figure 2. Time-resolved (TCSPC) photoluminescence of 2TV and 3TV in toluene solution. Recorded with excitation at 400 nm and detection at 427 nm (2TV) and 525 nm (3TV).

cence spectra for 2TV, 3TV, and 4TV are depicted in Figure 1b. Fluorescence measurements on the longer *n*TV oligomers (6TV, 8TV, and 12TV) reveal that excitation does not give rise to any detectable radiative decay ($\phi_{PL} \approx 0$). This behavior is consistent with the generally observed absence of fluorescence for PTVs.[29] The fluorescence intensity of the *n*TVs ($n = 2-4$), dissolved in 2-methyltetrahydrofuran (2-MeTHF) increased by almost 1 order of magnitude when going from solution at room temperature to a frozen matrix at 100 K. Both temperature and environmental rigidity, which inhibit twisting around the C=C bond, likely contribute to this enhancement.[30]

The singlet excited-state lifetimes (τ) as determined by time-correlated single-photon counting (TCSPC) at 295 K of 2TV (280 ps) and 3TV (1360 ps) differ significantly (Figure 2). Unfortunately, the fluorescence intensity of 4TV proved to be too low for its lifetime to be determined using TCSPC. Surprisingly, the radiative decay constant ($k_R = \phi_{PL}/\tau$) of 3TV is 1 order of magnitude less than that of 2TV (Table 1). In an attempt to understand this large difference, we estimated the radiative decay constant (k_R) and radiative lifetime (τ_R) of the three shorter oligomers in an independent way using the Strickler−Berg equation,[31] which provides a relation between the absorption intensities and fluorescence lifetimes of molecules

$$\frac{1}{\tau_R} = k_R = 2.880 \times 10^{-9} n^2 \langle \tilde{\nu}_f^{-3} \rangle_{Av}^{-1} \frac{g_l}{g_u} \int \frac{\epsilon}{\tilde{\nu}} \, d\tilde{\nu} \qquad (1)$$

Here, n is the refractive index of the solvent; $\tilde{\nu}$ and $\tilde{\nu}_f$ are the absorption and fluorescence wavenumbers, respectively; ϵ is the molar absorption coefficient; and g_l and g_u are the respective degeneracies of the lower and upper states (in our case, both states are nondegenerate; hence, $g_l = g_u = 1$). The analysis (Table 1) reveals that, according to the Strickler−Berg relation, the radiative decay (k_R) is almost constant for 2TV, 3TV, and 4TV, in contrast to the experimental results. Whereas the experimental and theoretical values of k_R are similar for 2TV, there is a significant overestimation of the k_R value for 3TV. We tentatively explain this difference by assuming that, for 3TV, the 2^1A_g state, which is not radiatively coupled to the ground state, is almost degenerate with the dipole-allowed 1^1B_u state. The increased fluorescence lifetime of 3TV, as compared to 2TV, could then result from mixing of the two degenerate states, which would reduce the rate of radiative decay. Such a crossing of the 2^1A_g and 1^1B_u states also explains the dramatic drop of *n*TV fluorescence quantum yield observed for $n > 3$, because, for longer *n*TVs, the dipole-forbidden 2^1A_g state is the lowest excited state. This behavior for *n*TVs bears a strong resemblance to that of linear oligo- and polyenes and related compounds for which it is well-established that the 2^1A_g state is the lowest excited state.[18,19]

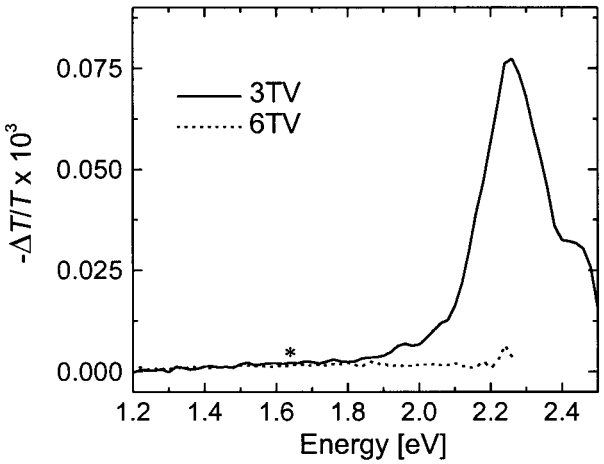

Figure 3. Fluorescence-corrected PIA spectra of 3TV (solid line) and 6TV (dotted line) in toluene, obtained by excitation at 458 and 488 nm, respectively. The asterisk indicates the position where the $T_n \leftarrow T_1$ absorption would be located for 6TV (see Figure 5).

To investigate the relaxation of the initially excited singlet state in more detail and to assess whether the nonradiative decay is due to intersystem crossing to a triplet state, we performed photoinduced absorption (PIA) measurements on the *n*TV molecules in solution. For 4TV, 6TV, 8TV, and 12TV, photoexcitation did not give rise to any photoinduced ($T_n \leftarrow T_1$) absorption, implying that the triplet excited state is not populated to any measurable extent. This is illustrated in Figure 3 for 6TV (dashed line), where the asterisk indicates the position where the 6TV $T_n \leftarrow T_1$ absorption would be expected, as will become clear in the following sections. In contrast, for 3TV, a photoinduced $T_n \leftarrow T_1$ absorption is observed at 2.28 eV. Hence, for 3TV, triplet excited state formation competes effectively with radiative and thermal decay after photoexcitation. The same would be expected for 2TV, but this compound rapidly deteriorated in the PIA experiment, which precluded recording the $T_n \leftarrow T_1$ spectrum.

Apparently, the lifetimes of the singlet excited states of 2TV and 3TV are sufficient to result in a nonzero quantum yield for fluorescence and intersystem crossing. For the longer compounds, 4TV being a borderline case, a very fast thermal decay (k_{TD}) apparently precedes any other decay mechanism from the photoexcited singlet state.

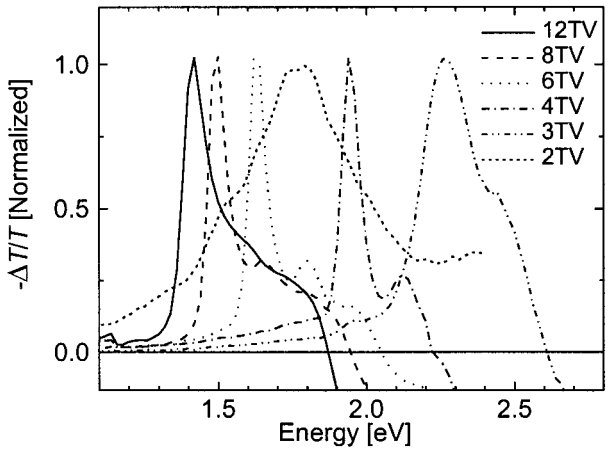

Figure 4. Normalized PIA spectra for mixtures of 2−12TV and MP−C_{60} in toluene at room temperature obtained via excitation of MP−C_{60}. The excitation wavelengths are 458 nm (12TV, 8TV, 6TV, and 4TV), 351/363 nm (3TV), and 488 nm (2TV). The spectrum for 2TV/MP−C_{60} corresponds to that of the MP−$C_{60}(T_1)$ state, whereas for the longer oligomers, the spectrum is that of the *n*TV(T_1) state. The negative signals originate from bleaching of the *n*TV ground state.

An estimate of the lifetime of 4TV can be obtained by combining the theoretical radiative decay constant k_R and the experimental fluorescence quantum yield [ϕ_{PL}(*n*TV)] (Table 1) to give the nonradiative decay constant k_{NR}

$$k_{NR} = \left(\frac{1 - \phi_{PL}(n\text{TV})}{\phi_{PL}(n\text{TV})}\right)k_R \qquad (2)$$

which subsequently provides the lifetime of the singlet excited state [τ(*n*TV)] via

$$\tau(n\text{TV}) = \frac{1}{k_R + k_{NR}} \qquad (3)$$

Table 1 shows that the nonradiative decay (k_{NR}) must increase strongly for 4TV to explain the extremely low fluorescence quantum yield. This results in very short excited-state lifetimes (on the order of picoseconds for 4TV).

2.2. Excitation of MP−C_{60} in *n*TV/MP−C_{60} Mixtures. Although the *n*TV triplet excited state [*n*TV(T_1)] cannot be attained directly via intersystem crossing from the *n*TV(S_1) state for $n > 3$, it might be populated indirectly via sensitization of the triplet state. For triplet energy transfer to occur, the T_1 level of the *n*TV should be lower in energy than the T_1 level of the sensitizer. In this study, we use MP−C_{60} as a triplet sensitizer. Excitation of MP−C_{60} in solution results in a weak fluorescence (ϕ_{PL} in toluene $= 6 \times 10^{-4}$)[34] at 1.74 eV and a long-lived (0.24 ms)[35] triplet excited state with a triplet energy at 1.50 eV.[36] The quantum yield for intersystem crossing from MP−$C_{60}(S_1)$ to MP−$C_{60}(T_1)$ is near unity, which is a desirable property for a sensitizer.[34] In the next sections, we describe experiments using photoexcited MP−C_{60} both as a triplet sensitizer of the *n*TV-(T_1) state in an apolar solvent and as an electron acceptor in the formation of a charge-separated state using a polar solvent.

2.2.1. Intermolecular Photoinduced Triplet Energy Transfer in Toluene. The PIA spectra shown in Figure 4 demonstrate that excitation of MP−C_{60} in mixtures of *n*TV/MP−C_{60} (molar ratio = 1:10) in toluene gives rise to the formation of *n*TV(T_1) triplet states via triplet energy transfer from the MP−$C_{60}(T_1)$ state for $n > 2$. The $T_n \leftarrow T_1$ absorption bands of the *n*TV oligomers are observed at lower energies with increasing oligomer length, in agreement with longer effective conjugation lengths (Table 2). All $T_n \leftarrow T_1$ absorptions are accompanied by a shoulder at higher energy, which has shifted by about 0.17−0.19 eV (1230−1450 cm^{-1}), consistent with a C=C stretch vibrational mode. For the 2TV/MP−C_{60} mixture, photoexcitation of MP−C_{60} results in the PIA spectrum of the MP−C_{60} triplet state, exhibiting an absorption band at 1.78 eV with a characteristic shoulder at 1.54 eV.[13] This implies that the triplet state of MP−C_{60} (1.50 eV) is energetically located below that of 2TV. The experiments demonstrate that MP−C_{60} can be effectively used as a triplet sensitizer for all *n*TVs, except for 2TV.

TABLE 2: Energies at Room Temperature of the *n*TV Absorption Bands, Singlet Excited States, Radical Cation Transitions, Triplet−Triplet Absorptions, and Triplet Excited State

	$S_1 \leftarrow S_0$[a] (eV)	$S_1 \leftarrow S_0$[b] (eV)	RC1 (eV)	RC2 (eV)	$T_n \leftarrow T_1$ (eV)	T_1[c] (eV)
2TV	3.45	3.23				1.52
3TV	2.85	2.60	1.08	1.66	2.28	1.32
4TV	2.56	2.29	0.85	1.40	1.94	1.23
6TV	2.29	2.03	0.63	1.13	1.63	1.14
8TV	2.18	1.91	0.53	1.04	1.50	1.10
12TV	2.11	1.85	0.46	1.00	1.42	1.06

[a] In CH_2Cl_2 at 295 K. [b] Determined from the decay of the low-energy vibronic transition in variable-temperature UV/vis spectra in 2-MeTHF (see Figure 8 and text). [c] Determined as the difference between the energy of the MP−$C_{60}(T_1)$ and the free energy for charge separation by assuming that the energies of triplet and charge-separated states in ODCB are equal.

2.2.2. Intermolecular Photoinduced Electron Transfer in ODCB. In more polar solvents, a charge-separated state will be stabilized as a result of the solvation of the radical ions formed and the screening of the Coulombic attraction of the positive and negative charges. To test the possibility of photoinduced electron transfer, we studied photoexcitation in a more polar solvent. Photoexcitation of MP−C_{60} in an *n*TV/MP−C_{60} mixture dissolved in ODCB indeed results in the formation of $n\text{TV}^{+\bullet}$ radical cations for $n > 2$ (Figure 5). In this reaction, the photoexcited MP−C_{60} molecule in the triplet state acts as an oxidizing agent toward the *n*TV oligomer in the ground state and is converted into the MP−$C_{60}^{-\bullet}$ radical anion with the concurrent formation of an $n\text{TV}^{+\bullet}$ radical cation. Two characteristic and intense $n\text{TV}^{+\bullet}$ absorptions can be observed, together with a less intense transition of the MP−$C_{60}^{-\bullet}$ radical anion at 1.24 eV (Figure 5). The lowest-energy band (RC1) of the $n\text{TV}^{+\bullet}$ absorptions is assigned to a transition from the lowest doubly occupied to the singly occupied electronic (polaron) level, and the higher-energy band (RC2) to a transition from the singly occupied level to the lowest unoccupied electronic level. As expected, the absorption bands of the two $n\text{TV}^{+\bullet}$ transitions (RC1 and RC2, Table 2) shift to lower energy with increasing chain length. The RC1 and RC2 transitions observed after photoexcitation of *n*TV/MP−C_{60} mixtures completely coincide with those previously obtained via chemical doping of the *n*TV molecules in dichloromethane solution using thianthrenium perchlorate as the oxidizing agent[37] and confirm the assignment to transitions of the $n\text{TV}^{+\bullet}$ radical cations.

Apart from the charge-separated state, the PIA spectra in Figure 5 also show the presence of *n*TV $T_n \leftarrow T_1$ absorptions. These absorption bands are slightly red-shifted (by about 0.02−0.04 eV) compared to those observed in toluene (Figure 4). Because the PIA measurements probe excited states in the micro- and millisecond time domains, at which thermodynamic

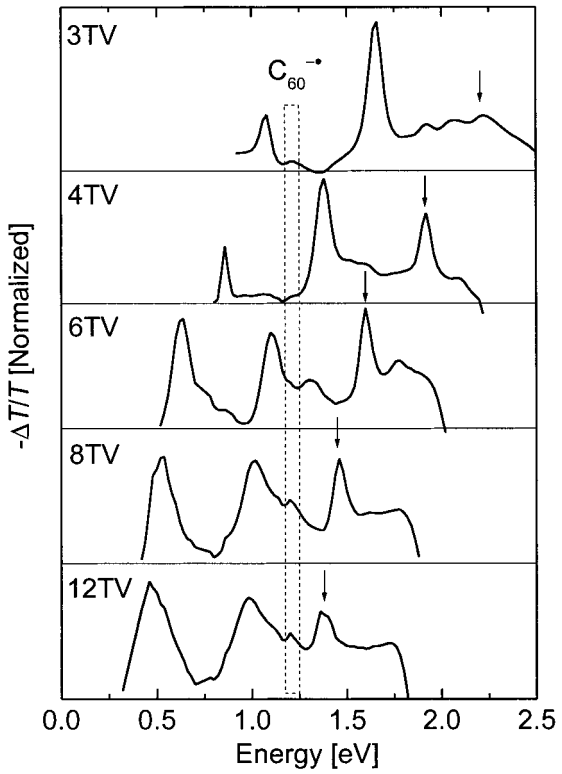

Figure 5. Normalized PIA spectra for mixtures of 3−12TV and MP−C_{60} in ODCB at room temperature obtained via excitation of MP−C_{60}. The excitation wavelengths are 458 nm (4TV, 6TV, 8TV, and 12TV) and 351/363 nm (3TV). The dotted rectangle denotes the transition of the MP−C_{60} radical anion. Excitation of a mixture of 2TV/MP−C_{60} at 488 nm yields the PIA spectrum corresponding to the MP−C_{60} triplet−triplet absorption. The *n*TV ($T_n \leftarrow T_1$) absorptions are indicated with arrows.

equilibrium is reached, we conclude that the energy levels of the charge-separated states and triplet excited states in ODCB are very close. A similar situation was recently reported for a quaterthiophene−fullerene dyad in benzonitrile.[20] For the 2TV/MP−C_{60} mixture in ODCB, photoexcitation of MP−C_{60} results in the PIA spectrum corresponding to the formation of MP−$C_{60}(T_1)$, analogous to the result in toluene.

2.2.3. Lifetime of the Triplet and Charge-Separated States. By varying the modulation frequency (ω) in the PIA experiment and recording the change in transmission ($-\Delta T$) at the position of the $T_n \leftarrow T_1$ transition, it possible to determine the lifetime of the triplet state (τ_m) by fitting the data to an analytical expression for monomolecular decay[38]

$$-\Delta T = \frac{Ig\tau_m}{\sqrt{1+\omega^2{\tau_m}^2}} \quad (4)$$

In eq 4, I is the intensity of the pump beam, and g is the efficiency of generating the photoinduced species.

In an analogous way, the lifetime (τ_b) of the *inter*molecularly charge-separated state can be obtained by fitting the changes in transmission ($-\Delta T$) of the radical cation band as a function of the modulation frequency to an expression for bimolecular decay[38]

$$-\Delta T = \sqrt{Ig/\beta}\left(\frac{\alpha \tanh \alpha}{\alpha + \tanh \alpha}\right) \quad (5)$$

Here, β is the bimolecular decay constant, and $\alpha = \pi/(\omega\tau_b)$,

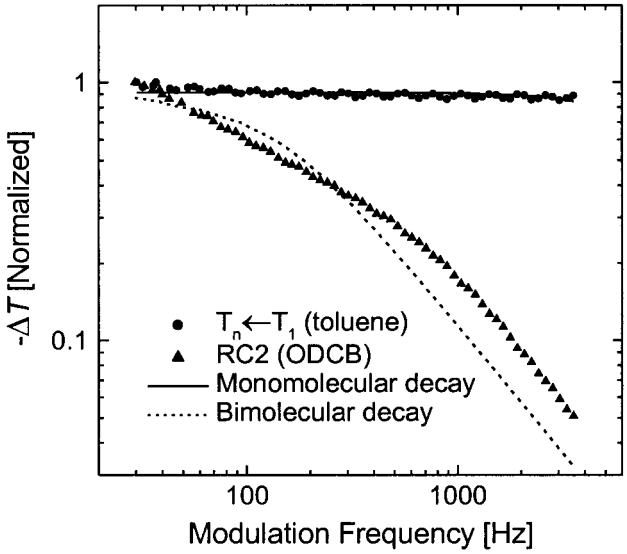

Figure 6. Normalized modulation frequency dependence of the PIA spectra of 4TV recorded at 1.94 eV ($T_n \leftarrow T_1$) in toluene (circles) and at 1.37 eV (RC2 transition) in ODCB (triangles) with excitation at 458 nm. The lines represent least-squares fits to the expressions for monomolecular decay (solid line, eq 4) and bimolecular decay (dashed line, eq 5).

with $\tau_b = (gI\beta)^{-0.5}$, is the bimolecular lifetime under steady-state conditions. It is important to note that τ_b depends on the experimental conditions such as concentration and pump beam intensity.

Figure 6 shows the normalized change in transmission ($-\Delta T$) as a function of the modulation frequency for the $T_n \leftarrow T_1$ transition of 4TV in toluene and for the RC2 transition of $4TV^{+\bullet}$ in ODCB. The results for 4TV are characteristic of the behavior of all *n*TV oligomers ($n > 2$). The change in transmission of the RC2 band decays over more than one decade in the recorded frequency range, whereas the change in transmission of the $T_n \leftarrow T_1$ transition remains essentially constant. These observations are characteristic for relatively long-lived and short-lived species, respectively. The frequency-dependent changes of $-\Delta T$ for all *n*TV(T_1) states are small in the recorded frequency range, which implies lifetimes $\tau_m \leq 0.1-0.2$ ms, close to the 0.24 ms MP−$C_{60}(T_1)$ lifetime.[13] For the intermolecularly charge-separated state, the lifetime τ_b is much longer, on the order of 5−15 ms, and comparable to values reported for intermolecularly charge-separated states in mixtures of MP−C_{60} and *n*Ts and *n*PVs.[13,14] However, Figure 6 shows that the bimolecular decay expression fits quite inadequately to the ΔT data. This occurs for all frequency dependencies of ΔT recorded for the radical cation bands. The observed continuous decrease of ΔT points to a distribution of lifetimes, which might be related to the fact that some decomposition occurs in ODCB in the PIA experiments.[39]

2.2.4. Energetic Considerations for Intermolecular Energy and Electron Transfer. The change in free energy for charge separation (ΔG_{CS}) for a photoinduced electron transfer in solution can be semiquantitatively described by the Weller equation[40]

$$\Delta G_{cs} = e[E_{ox}(D) - E_{red}(A)] - E_{00} - \frac{e^2}{4\pi\epsilon_0\epsilon_s R_{CC}} - \frac{e^2}{8\pi\epsilon_0}\left(\frac{1}{r^+}+\frac{1}{r^-}\right)\left(\frac{1}{\epsilon_{ref}}-\frac{1}{\epsilon_s}\right) \quad (6)$$

In eq 6, $E_{ox}(D)$ and $E_{red}(A)$ are, respectively, the oxidation and

TABLE 3: Oxidation Potential (E_{ox}), Radius of Positive Ion (r^+), Center-to-Center Distance of the Positive and Negative Charges in the Charge-Separated State (R_{CC}), and Change in Free Energy for Charge-Separation (ΔG_{CS}) Relative to the MP−C_{60}(S_1) and MP−C_{60}(T_1) Levels in Toluene and ODCB, Respectively

				MP−C_{60}(S_1)		MP−C_{60}(T_1)	
	E_{ox} (V)	r^+ (Å)	R_{CC} (Å)	ΔG_{CS}^{Tol} (eV)	ΔG_{C}^{ODCB} (eV)	ΔG_{CS}^{Tol} (eV)	ΔG_{CS}^{ODCB} (eV)
2TV	0.89	3.79	∞[a]	0.78	−0.24	1.04	0.02
3TV	0.68	4.32	∞[a]	0.50	−0.44	0.76	−0.18
4TV	0.59	4.75	∞[a]	0.36	−0.53	0.62	−0.27
6TV	0.50	5.42	∞[a]	0.22	−0.62	0.48	−0.36
8TV	0.46	5.69	∞[a]	0.14	−0.66	0.40	−0.40
12TV	0.42	6.82	∞[a]	0.05	−0.70	0.31	−0.44
C_{60}−2TV	0.89	3.79	9.50[b]	0.14	−0.39	0.40	−0.13
C_{60}−3TV	0.68	4.32	12.30[b]	0.01	−0.56	0.27	−0.30
C_{60}−4TV−C_{60}	0.59	4.75	15.30[b]	−0.03	−0.63	0.23	−0.37

[a] *Inter*molecular electron transfer. [b] *Intra*molecular electron transfer.

reduction potentials of the donor and acceptor moieties in a solvent with relative permittivity ϵ_{ref}. E_{00} is the energy of the excited state from which electron transfer occurs; r^+ and r^- are the radii of the positive and negative ions, respectively; ϵ_s the relative permittivity of the solvent; and e and ϵ_0 are the electron charge and the vacuum permittivity, respectively. R_{CC} is the center-to-center distance of the positive and negative ions, which is set to infinity for *inter*molecular electron transfer, as the ions can diffuse in solution. The oxidation potentials of the *n*TVs (Table 3)[21] and the reduction potential of MP−C_{60} (E_{red} = −0.70 V versus SCE) have been determined in dichloromethane (ϵ_{ref} = 8.93). Because intermolecular electron transfer occurs from the MP−C_{60}(T_1) state, E_{00} is 1.50 eV.[36] The radius of the negative ion of MP−C_{60} was set to r^- = 5.6 Å, based on the density of C_{60}.[34,41] After determination of the molar volume of the unsubstituted *n*TV molecules (n = 2−12) with molecular modeling, the radii of the positive ions, r^+, could be estimated (Table 3). We are aware that taking a single radius for a one-dimensionally extended molecule is a simplification of the actual situation. Moreover, in this approach, we chose to ignore the β- and β'-hexyl side chains, because the positive charge is confined to the conjugated segment. Table 3 shows the resulting estimated change in free energy for *inter*molecular charge separation relative to both the MP−C_{60}(S_1) and MP−C_{60}(T_1) energy levels. It can be seen that, in polar media, e.g., ODCB, *inter*molecular charge separation in *n*TV/MP−C_{60} solution mixtures is energetically feasible for n > 2, after photoexcitation of MP−C_{60} and intersystem crossing to MP−C_{60}(T_1). In apolar media, e.g., toluene, the *inter*molecularly charge-separated state levels are energetically located above MP−C_{60}(T_1) for all *n*TVs.

The calculated energy levels for the charge-separated state of the *n*TV/MP−C_{60} mixtures (n = 2−12) (equal to ΔG_{CS} + 1.50 eV) are depicted in Figure 7, together with the *n*TV(S_1), MP−C_{60}(S_1), and MP−C_{60}(T_1) levels. Because the *n*TV(S_1) energy could not be determined from fluorescence measurements for n > 4, they have been estimated from the temperature dependence of the *n*TV UV/vis absorption spectra in 2-MeTHF (shown in Figure 8a for 4TV). The absorption spectra in 2-MeTHF demonstrate a significant red shift upon going to lower temperatures, accompanied by an increased resolution of the vibronic bands. The high vibronic resolution of the *n*TV transitions at 90 K is illustrated in Figure 8b. The observed concentration *in*dependence of the changes with temperature (not shown) confirms their *intra*molecular origin, e.g., via an increased degree of planarity with decreasing temperature. The

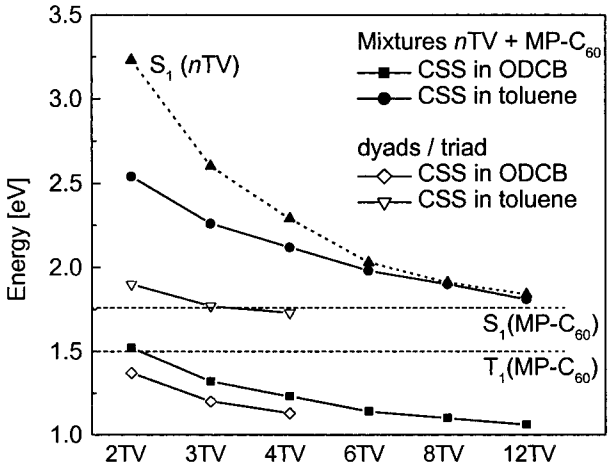

Figure 7. Charge-separated state energies as determined via eq 6 for the *n*TV/MP−C_{60} systems as functions of *n*. The upper curve (▲) represents the singlet excited state *n*TV(S_1) level (see Figure 8, Table 2, and text). The horizontal dashed lines are the MP−C_{60}(S_1) and MP−C_{60}(T_1) energy levels. The calculated free energies of the intermolecularly charge-separated state relative to the MP−C_{60}(T_1) level for *n*TV/MP−C_{60} mixtures in toluene and ODCB are represented by solid circles (●) and solid squares (■), respectively; those of the intramolecularly charge-separated states for C_{60}−2TV, C_{60}−3TV, and C_{60}−4TV−C_{60} in toluene and ODCB are indicated by open down triangles (▽) and diamonds (◊), respectively.

energy of the low-energy (0−0) vibronic decreases as a function of the reciprocal temperature (inset of Figure 8a) and reaches a constant value. The asymptotic values were chosen to approximate the *n*TV(S_1) energy level (Table 2).

Both Table 3 and Figure 7 show that the experimentally observed photoinduced energy- and electron-transfer reactions in the *n*TV/MP−C_{60} mixtures are in full agreement with the theoretical approximations according to the Weller equation. From the PIA experiments in ODCB, we concluded that the energy levels of the *n*TV triplet and charge-separated states are very similar. We assume that the *n*TV triplet energies will only change to a minor extent when the solvent is changed to toluene. Hence, we consider the energy values of the charge-separated states in ODCB (Table 3, solid squares in Figure 7) to be equal to the *n*TV(T_1) energy levels in both ODCB and toluene. This conjecture corroborates the formation of *n*TV(T_1) after photoexcitation of MP−C_{60} for n > 2 in toluene and of MP−C_{60}(T_1) for n = 2.

In Figure 9, the possible routes following photoexcitation of MP−C_{60} in *n*TV/MP−C_{60} mixtures are depicted schematically. For n > 2, we assume that, in toluene, the MP−C_{60}(S_1) state decays via intersystem crossing (k'_{ICS}) to the MP−C_{60}(T_1) state, which is subsequently quenched by triplet energy transfer (k_{TT}) to the *n*TV(T_1) state. In ODCB, MP−C_{60}(T_1) formation is followed by a simultaneous triplet energy transfer to *n*TV(T_1) and oxidation of the *n*TV moiety, resulting in charge separation (k_{CS}^{inter}).

2.2.5. Transition Energies as a Function of the nTV Chain Length. Figure 10 reveals that the transition energies of the *n*TVs discussed so far shift linearly with the reciprocal number of double bonds (1/*N*) for n < 12 or N < 35. The ground-state absorption ($S_1 \leftarrow S_0$), triplet absorption ($T_n \leftarrow T_1$), and radical cation transitions (only RC2 is depicted) shift with approximately equal slopes, denoting comparable changes in the degree of delocalization with chain extension. For these transitions, it can be seen that the deviation from linearity, indicating a convergence limit, only starts at a high number of double bonds

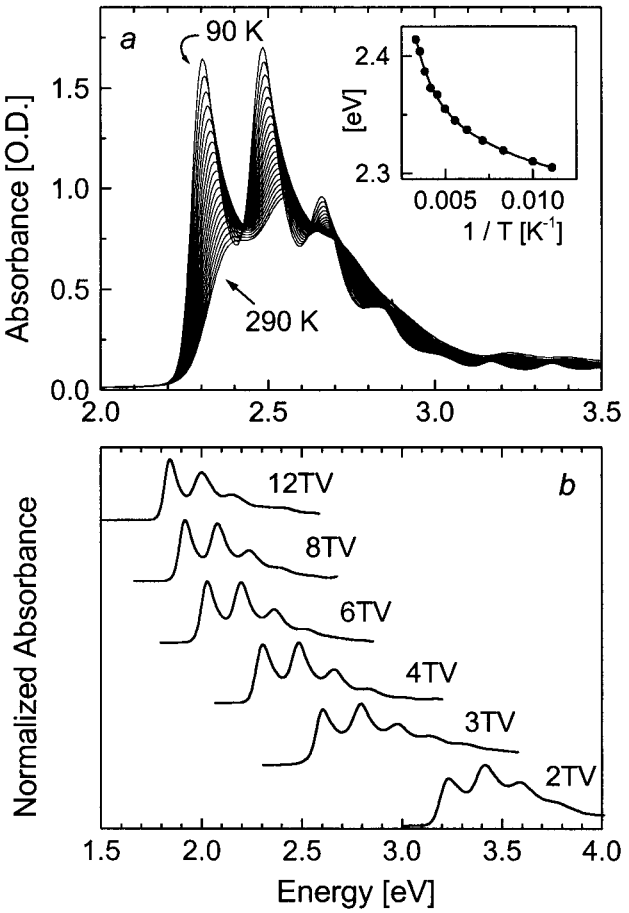

Figure 8. (a) UV/vis absorption spectra of 4TV in 2-MeTHF as a function of the temperature (from 290 to 90 K in steps of 10 K). The spectra are not corrected for volume changes upon cooling. The inset of a shows the position of the low-energy vibronic (0−0) transition as a function of the reciprocal temperature and an exponential decay fit through the data points. (b) Spectra at 90 K of 2−12TV in 2-MeTHF.

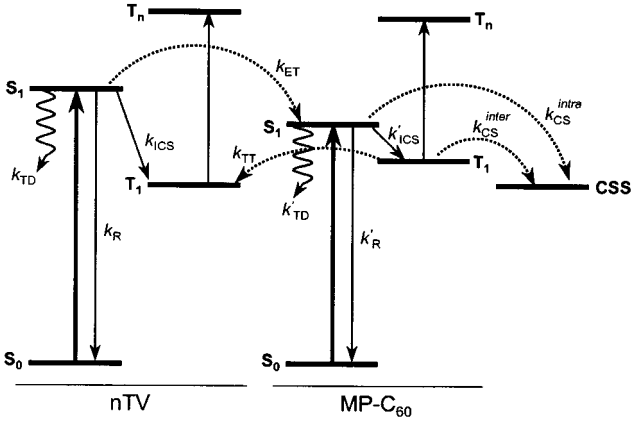

Figure 9. Diagram describing the energy levels of singlet (S_0 and S_1) and triplet states (T_1 and T_n) of the *n*TV molecules and MP−C_{60} and the possible interconversions between them. k_R and k'_R are the radiative rate constants for the *n*TVs and MP−C_{60}, respectively. Similarly, k_{TD} and k'_{TD}, denote the thermal decay rate constants, and k_{ICS} and k'_{ICS} the rate constants for intersystem crossing. k_{ET} and k_{TT} represent the rate constants for singlet energy transfer and triplet energy transfer, respectively; k_{CS}^{inter} and k_{CS}^{intra} are the rate constants for inter- and intramolecular charge separation, respectively.

($N \approx 35$, 12TV), which is significantly higher than the convergence limit in the case of *n*Ts and *n*PVs.[22] The slope of the triplet energy (T_1) against $1/N$ is noticeably flatter than those

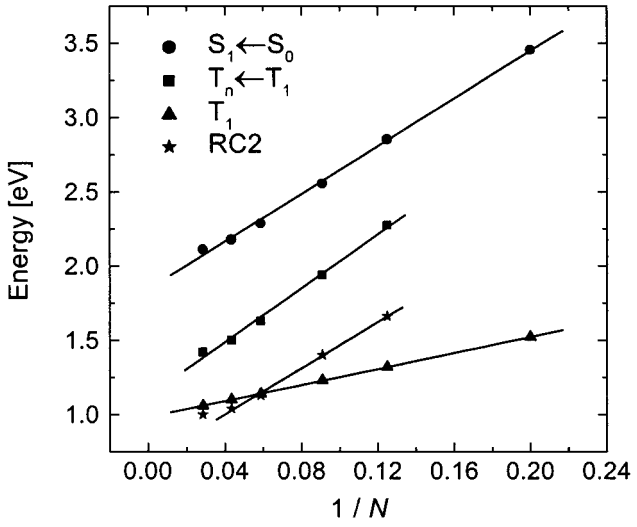

Figure 10. Absorption maxima of the $S_1 \leftarrow S_0$ (circles), $T_n \leftarrow T_1$ (squares), and RC2 (stars) transitions and energy of the triplet excited state (triangles) as functions of the reciprocal number of double bonds ($1/N$) for 2−12TV. All values are determined in toluene, except for RC2 (ODCB). The solid lines are linear fits.

of the optical transitions, and a perfect linearity is observed for the whole series, without any indication of a convergence limit. These observations should be interpreted with care, as the T_1 energies are based on the Weller equation (eq 6), whereas the values for the optical transitions in Figure 10 were determined experimentally. However, the trends suggest that the T_1 state is rather localized, in agreement with previous propositions.[42]

2.3. *Intra*molecular Photoinduced Processes in Covalently Linked C_{60}−*n*TV Systems: C_{60}−2TV, C_{60}−3TV, and C_{60}−4TV−C_{60}. By covalently linking the *n*TVs and MP−C_{60}, *intra*molecular photoinduced processes can be examined. We investigated the behavior upon photoexcitation of three covalently linked C_{60}−*n*TV (acceptor−donor) molecules: C_{60}−2TV, C_{60}−3TV, and C_{60}−4TV−C_{60} (Chart 2) in apolar (toluene) and polar (ODCB) solvents.

2.3.1. Ground-State Absorption Spectra. The absorption spectra of C_{60}−2TV, C_{60}−3TV, and C_{60}−4TV−C_{60} closely correspond to superpositions of the individual spectra of the corresponding *n*TV and MP−C_{60} moieties, as illustrated in Figure 11 for C_{60}−4TV−C_{60}. However, a small red shift of the 4TV absorption in the triad is observed compared to that of the bare 4TV, possibly resulting from the presence of two α,ω-carbon atoms. Despite the small shift, the spectra show no indications of electron transfer between donor and acceptor in the ground state.

2.3.2. Energetics of Intramolecular Energy and Electron Transfer. To determine the free energy change accompanying the formation of an *intra*molecularly charge-separated state, we again make use of the Weller equation (eq 6). The R_{CC} term, which represents the center-to-center distance of the positive and negative ions, now becomes an important parameter. Via molecular modeling, we determined R_{CC} values, and we use the E_{ox} values as determined for the corresponding unsubstituted *n*TVs.[21,43] The main parameters involved in the Weller equation, as well as the calculated change in free energy of *intra*molecular charge separation relative to the MP−C_{60}(T_1) state in both toluene and ODCB, are collected in Table 3. The charge-separated state energies for the C_{60}−*n*TV(−C_{60}) molecules are plotted as functions of the *n*TV chain length in Figure 7 (open symbols). A comparison with the charge-separated state energies in the corresponding MP−C_{60}/*n*TV *mixtures* (Figure 7, solid

TABLE 4: Fluorescence Quenching of the Dyads and Triad [$\phi_{PL}(n\text{TV})/\phi_{PL}$ and $\phi_{PL}(\text{MP-c}_{60})/\phi_{PL}$] in Solution and Rate Constants for Singlet Energy Transfer (k_{ET})[a] and Charge Separation (k_{CS}^{intra})[b]

	toluene				ODCB	
	$\phi(n\text{TV})/\phi$	k_{ET} (s^{-1})	$\phi(\text{MP}-\text{C}_{60})/\phi$	k_{CS}^{intra} (s^{-1})	$\phi(\text{MP}-\text{C}_{60})\phi$	k_{CS}^{intra} (s^{-1})
$\text{C}_{60}-2\text{TV}$	750	2.7×10^{12}	1		9	0.6×10^{10}
$\text{C}_{60}-3\text{TV}$	620	4.6×10^{11}	16	1.0×10^{10}	33	2.2×10^{10}
$\text{C}_{60}-4\text{TV}-\text{C}_{60}$	80		86	5.9×10^{10}	133	9.1×10^{10}

[a] According to eq 7. [b] According to eq 8.

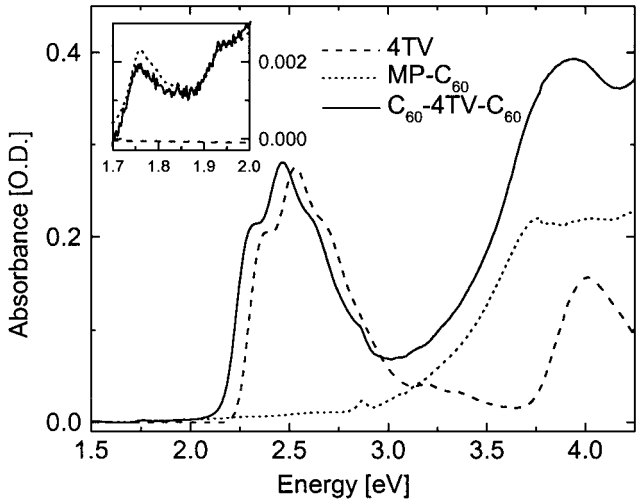

Figure 11. Absorption spectra of 4TV (1×10^{-5} M, dashed line), $\text{MP}-\text{C}_{60}$ (2×10^{-5} M, dotted line), and $\text{C}_{60}-4\text{TV}-\text{C}_{60}$ (1×10^{-5} M, solid line) in toluene. The inset shows a magnification of the 1.7−2 eV region, with the 0−0 vibronic transition of the $\text{MP}-\text{C}_{60}$ $S_1 \leftarrow S_0$ band.

symbols) reveals that, in both toluene and ODCB, *intra*molecular electron transfer is energetically more favorable than *inter*molecular electron transfer, as a result of the decreased distance between the oppositely charged species. Hence, it is safe to assume that *intra*molecular electron transfer is allowed in cases where *inter*molecular electron transfer occurs.

2.3.3. Fluorescence Spectra of the $C_{60}-n$TVs in Toluene and ODCB. When excited at the wavelength of maximum absorption of the *n*TV moiety, the *n*TV fluorescence of the $\text{C}_{60}-n\text{TV}-(-\text{C}_{60})$ molecules dissolved in toluene is strongly quenched with respect to the emission of the unsubstituted *n*TV oligomers (Table 4). This quenching is consistent with a fast decay of the $n\text{TV}(S_1)$ state via singlet energy transfer (Figure 9, k_{ET}), as previously reported for *n*Ts and *n*PVs covalently bonded to C_{60}.[13,14] These and related studies reveal that *intra*molecular singlet energy transfer from a photoexcited conjugated oligomer to a covalently bonded fullerene moiety occurs on very short time scales ($k_{ET} > 10^{12}$ s^{-1}).[6,11−20] In fact, the energy-transfer reaction was recently timed with <10-fs pulses for a fullerene−novithiophene−fullerene triad to be $k_{ET} = 1.05 \times 10^{13}$ s^{-1}.[15b]

The ratio of the *n*TV fluorescence of unsubstituted and C_{60}-substituted *n*TVs [$\phi_{PL}(n\text{TV})/\phi_{PL}$] and the S_1 lifetimes of the pristine *n*TV oligomers [$\tau(n\text{TV})$, Table 1] provide an indication for the rate constant of the singlet energy-transfer reaction via

$$k_{ET} = \left[\frac{\phi_{PL}(n\text{TV})}{\phi_{PL}} - 1\right]/\tau(n\text{TV}) \qquad (7)$$

The resulting values for k_{ET} (Table 4) indicate that this singlet energy transfer is indeed extremely fast and reduces the $n\text{TV}(S_1)$ lifetime for $n = 2$ and 3 to the (sub)picosecond time scale.

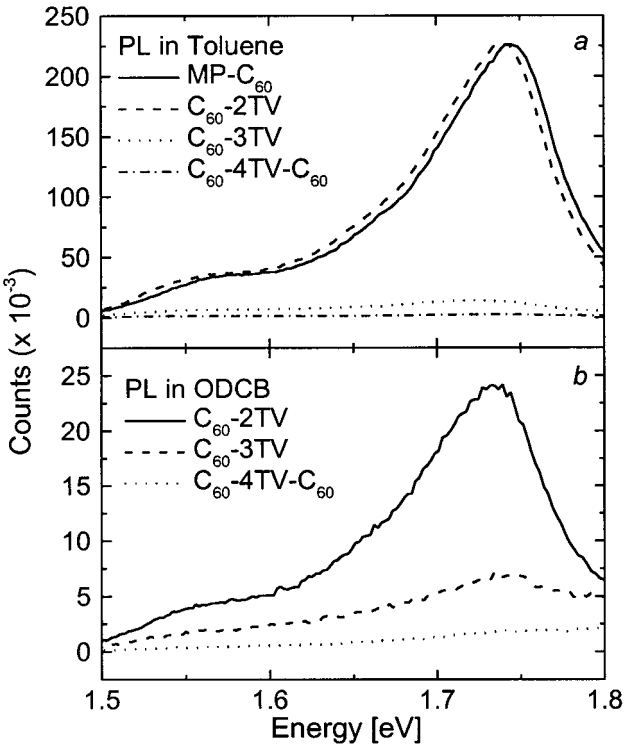

Figure 12. Fluorescence spectra of $\text{MP}-\text{C}_{60}$, $\text{C}_{60}-2\text{TV}$, $\text{C}_{60}-3\text{TV}$, and $\text{C}_{60}-4\text{TV}-\text{C}_{60}$ in (a) toluene and (b) ODCB. The spectra were recorded at 295 K. The intensity of the spectra was independent of the excitation wavelength, provided that the optical density of the samples was 0.1 at the excitation wavelength. Fluorescence spectra were not corrected for the response of the detection system.

The fast singlet energy-transfer reaction produces the singlet excited state of the fullerene moiety, similarly to direct photoexcitation. It is well-established that the singlet excited state of $\text{MP}-\text{C}_{60}$ molecules results in a weak fluorescence at 1.74 eV in solution, with a reported quantum yield of 6×10^{-4} in toluene.[34] Figure 12a shows the fullerene fluorescence spectra of $\text{MP}-\text{C}_{60}$ and the three $\text{C}_{60}-n\text{TV}(-\text{C}_{60})$ covalently linked systems in toluene. It is essential to note that the intensity of the spectra was independent of the excitation wavelength for all compounds, provided that the optical density at the excitation wavelength was identical. In particular, for the $\text{C}_{60}-n\text{TV}(-\text{C}_{60})$ compounds, no differences in intensity were observed when either the *n*TV moiety or the fullerene moiety was excited preferentially. This result provides unambiguous evidence of the fast singlet energy-transfer reaction from *n*TV to the fullerene in the dyads and triad in toluene solution.

For the two longer oligomers, the fluorescence of the $\text{MP}-\text{C}_{60}$ moiety in $\text{C}_{60}-n\text{TV}(-\text{C}_{60})$ is significantly reduced compared to that of the free $\text{MP}-\text{C}_{60}$ molecule: whereas no quenching was found for $\text{C}_{60}-2\text{TV}$, quenchings of 94% for $\text{C}_{60}-3\text{TV}$ and of 99% for $\text{C}_{60}-4\text{TV}-\text{C}_{60}$ were observed (Figure 12a, Table 4). Because the quenching is independent of the

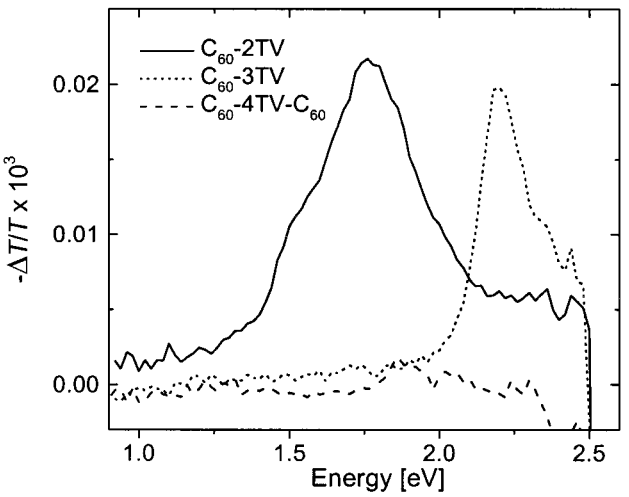

Figure 13. PIA spectra of C_{60}−2TV (solid line), C_{60}−3TV (dotted line), and C_{60}−4TV−C_{60} (dashed line) in toluene. The excitation wavelength is 488 nm.

excitation wavelength, a rapid relaxation of the MP−C_{60}(S_1) state must be invoked to explain this effect.

In the more polar solvent, ODCB, excitation of the *n*TV moieties in the dyads/triad again shows a residual but strongly quenched *n*TV emission. In this solvent, MP−C_{60} emission is very weak, and quenching is now observed for all C_{60}−*n*TV-(−C_{60}) systems: 89% for C_{60}−2TV, 97% for C_{60}−3TV, and virtually 100% for C_{60}−4TV−C_{60} (Figure 12b, Table 4). Because the residual emission of the *n*TV moiety in ODCB is similar to that observed in toluene, we assume that the process that completely quenches the emission of the MP−C_{60} moiety in ODCB originates not from the short-lived *n*TV(S_1) state, but rather from the MP−C_{60}(S_1) state. Before explaining the origin of the quenching and its dependence on solvent polarity, we describe the results of PIA experiments of the C_{60}−*n*TVs in solution.

2.3.4. Photoinduced Absorption Spectra of the C_{60}−nTVs. The PIA spectra recorded in toluene (Figure 13) show the MP−C_{60} ($T_n \leftarrow T_1$) transition for C_{60}−2TV and the 3TV ($T_n \leftarrow T_1$) transition for C_{60}−3TV. For C_{60}−4TV−C_{60}, no PIA transition can be distinguished from the noise. In ODCB (not shown), a weak ($-\Delta T/T \approx 5 \times 10^{-6}$) MP−$C_{60}$ ($T_n \leftarrow T_1$) transition just above the detection limit is observed for C_{60}−2TV, whereas for C_{60}−3TV and C_{60}−4TV−C_{60}, no signals were observed.

2.3.5. Intramolecular Energy versus Electron Transfer in ODCB. Recently, a two-step mechanism for photoinduced charge separation, involving a fast singlet energy transfer followed by electron transfer, was proposed for C_{60}-substituted dyads and triads containing *n*T and *n*PV moieties in polar solvents.[13−15] For the C_{60}−*n*TVs in ODCB, the charge-separated state (CSS) is the energetically most favorable excited state, on the basis of the predictions of the Weller equation (eq 6, Table 3, Figure 7). Fluorescence studies reveal almost complete quenching of both *n*TV and MP−C_{60} emission in the covalently linked systems in ODCB (relative to the quantum yields of pure *n*TV and MP−C_{60}) (Figure 12b), and PIA measurements demonstrate the lack of any detectable photoinduced absorption. Because we observe similar quenchings of the *n*TV fluorescence in both toluene and ODCB and because the singlet energy transfer, which was clearly established to occur in toluene from the constant fullerene emission at different excitation wavelengths, is not strongly dependent on the polarity of the solvent, we propose that the present observations are consistent with a two-step mechanism for charge separation in ODCB after photoexcitation of the *n*TV moiety: A very fast singlet energy transfer to MP−C_{60}(S_1) quenches the *n*TV ($S_1 \leftarrow S_0$) emission ($k_{ET} \gg k_R$, Figure 9), and subsequently, the MP−C_{60} ($S_1 \leftarrow S_0$) emission is quenched by a very rapid intramolecular electron transfer ($k_{CS}^{intra} \gg k_R'$, Figure 9), yielding an *intra*molecularly charge-separated ion pair ($C_{60}^{-\bullet}$ − *n*$TV^{+\bullet}$). The fact that the *n*$TV^{+\bullet}$ and MP−$C_{60}^{-\bullet}$ radical ion transitions do not appear in the PIA spectrum is consistent with a subsequent fast *intra*molecular recombination, resulting in *intra*molecular CSS lifetimes that are too short to give rise to a substantial steady-state concentration (in general, species with lifetimes less than ∼10 μs are below the near-steady-state PIA detection limit of $-\Delta T/T \approx 10^{-6}$). For most covalent donor−acceptor systems involving fullerene derivatives, the CSS lifetime is limited to the sub-nanosecond time domain.[15,25] In the case of C_{60}−2TV in ODCB, the MP−C_{60}(T_1) and CSS energy levels are quite close (Figure 7), which apparently results in an equilibrium between the two species and, hence, in a weak MP−C_{60} ($T_n \leftarrow T_1$) transition in the PIA spectrum.

The rate constant for the intramolecular electron-transfer reaction (k_{CS}^{intra}) in which an electron is transferred from the *n*TV moiety in the ground state to the MP−C_{60} moiety in the singlet excited state can be determined from the singlet excited-state lifetime of MP−C_{60} (1.45 ns) and the quenching ratios via

$$k_{CS}^{intra} = \left[\frac{\phi_{PL}(MP-C_{60})}{\phi_{PL}}\right]/\tau(MP-C_{60}) \qquad (8)$$

and the resulting values (Table 4) show that the rate increases from 0.6×10^{10} s^{-1} for C_{60}−2TV to 9.1×10^{10} s^{-1} for C_{60}−4TV−C_{60}.

2.3.6. Intramolecular Energy versus Electron Transfer in Toluene. Photoexcitation of the C_{60}−*n*TV(−C_{60}) molecules in toluene initially produces the MP−C_{60}(S_1) state, either via direct excitation or via singlet energy transfer (k_{ET}) from the *n*TV(S_1) state, which occurs with a quantum efficiency near unity. We show below that the decay process of this MP−C_{60}(S_1) state depends on the length of the *n*TV moiety.

The CSS energy levels of the C_{60}−*n*TVs in toluene are located above the MP−C_{60}(T_1) level (Figure 7), which, in turn, is above the *n*TV(T_1) level (solid squares, Figure 7) for C_{60}−3TV, and for C_{60}−4TV−C_{60}, the *n*TV(T_1) levels are energetically equivalent to the levels for *inter*molecular charge separation in ODCB. Hence, the experimental observation of the MP−C_{60} and 3TV ($T_n \leftarrow T_1$) transitions in the PIA spectra of C_{60}−2TV and C_{60}−3TV (Figure 13), respectively, is in agreement with the energetic expectations, as they correspond to the lowest-energy excited state for each system.

The significant quenching of the MP−C_{60} fluorescence in toluene for C_{60}−3TV and C_{60}−4TV−C_{60} and the absence thereof for C_{60}−2TV (Figure 12), as well as the lack of any detectable PIA signal for C_{60}−4TV−C_{60} (Figure 13), have to be clarified. For C_{60}−3TV and C_{60}−4TV−C_{60} the energy levels calculated for the charge-separated state in toluene are almost equal to or below the MP−C_{60}(S_1) level (Figure 7, Table 3), whereas that for C_{60}−2TV is significantly higher in energy. In combination with the fullerene emission quenching observed for C_{60}−3TV and C_{60}−4TV−C_{60} and the absence of such quenching for C_{60}−2TV, we therefore propose that an *intra*molecularly charge-separated state (k_{CS}^{intra}, Figure 9) is formed in toluene for C_{60}−3TV and C_{60}−4TV−C_{60}, but not for C_{60}−2TV. Because the charge-separated state is not the lowest-energy

excited state, its formation from the MP−C_{60}(S_1) state in C_{60}−3TV and C_{60}−4TV−C_{60} must be kinetically favored in comparison to fluorescence or intersystem crossing to the (lower-lying) triplet state. The rate constants for the intramolecular charge separation in toluene can be determined using eq 8, giving $k_{CS}^{intra} = 1.0 \times 10^{10}$ s^{-1} for C_{60}−3TV and 5.9×10^{10} s^{-1} for C_{60}−4TV−C_{60}.

Although the PIA spectra (Figure 13) *do* show the MP−C_{60}-(T_1) and 3TV(T_1) states for C_{60}−2TV and C_{60}−3TV, respectively, they do not provide a quantitative estimate of the overall quantum yields of MP−C_{60}(T_1) and 3TV(T_1) formation. In the case of C_{60}−4TV−C_{60}, where the CSS energy level is lower than the MP−C_{60}(S_1) level (Figure 7), no PIA signal could be detected (Figure 13). This is consistent with a fast *intra*molecular recombination of charges to the ground state, similar to the observations in ODCB. Apparently, this recombination to the ground state is faster than a possible decay of the *intra*molecularly CSS to the lower-lying triplet excited states [e.g., *n*TV-(T_1) for C_{60}−3TV and C_{60}−4TV−C_{60}].

To summarize, we propose that, in toluene, two processes occur simultaneously after initial photoexcitation of the *n*TV moiety and ultrafast *intra*molecular singlet energy transfer to MP−C_{60}(S_1): (a) formation of an *intra*molecularly charge-separated state (k_{CS}^{intra}, Figure 9), followed by a rapid recombination of charges to the ground state, and (b) fluorescence and intersystem crossing to MP−C_{60}(T_1), possibly followed by triplet energy transfer to *n*TV(T_1). The relative rates of these processes depend on the relative positions of the MP−C_{60}(S_1) and CSS levels. Because, in C_{60}−4TV−C_{60}, the CSS energy level is favored compared to the MP−C_{60}(S_1) level (Figure 7, Table 3), a is the dominant route. For C_{60}−3TV, the partial quenching of the MP−C_{60} fluorescence (Figure 12a, Table 4) is attributed to process a, whereas the remaining fluorescence and the triplet-state PIA spectra (Figure 13) are the clear signatures of the contribution of process b. Process b is the dominant relaxation pathway for C_{60}−2TV.

3. Conclusions

The photoinduced energy- and electron-transfer processes between oligothienylenevinylenes (*n*TV, $n = 2$, 3, 4, 6, 8, and 12) and *N*-methylfulleropyrrolidine (MP−C_{60}) (Chart 1) have been investigated in apolar and polar media. Excitation of the longer *n*TV oligomers ($n > 3$) was shown to result in an ultrashort-lived *n*TV(S_1) state because of a fast thermal decay, kinetically preventing fluorescence, intersystem crossing, and direct electron transfer from taking place from this *n*TV(S_1) state. However, the *n*TV(T_1) state could be populated indirectly via energy transfer using MP−C_{60} as a triplet sensitizer. In toluene ($\epsilon = 2.38$), this *inter*molecular triplet energy transfer occurs for $n > 2$, and we were able to record for the first time *n*TV $T_n \leftarrow T_1$ spectra as a function of chain length. In a more polar solvent, an *inter*molecularly charge-separated state is formed via excitation of MP−C_{60}, intersystem crossing to the MP−C_{60}(T_1) state, and subsequent electron transfer from *n*TV(S_0) to this triplet state. Accordingly, in *o*-dichlorobenzene (ODCB, $\epsilon = 9.93$), the MP−C_{60}(T_1) state acts as an oxidizing agent, resulting in the formation of a metastable radical ion pair (nTV$^{+\bullet}$ + MP−$C_{60}^{-\bullet}$) for $n > 2$, while simultaneous triplet energy transfer produces the *n*TV(T_1) state. Our experiments indicate that, in ODCB, the energy levels of the *n*TV(T_1) state and the *inter*molecularly charge-separated state are nearly degenerate for $n > 2$. For $n = 2$, the MP−C_{60}(T_1) state is the lowest excited state in both solvents. The energies of the electronic transitions of the ground state ($S_1 \leftarrow S_0$), the triplet state ($T_n \leftarrow T_1$), and the radical cations exhibit similar degrees of dispersion as a function of the reciprocal number of *n*TV double bonds. In contrast, the slope of a plot of the T_1 energy versus $1/N$ is significantly lower, consistent with a rather localized triplet excited state.

*Intra*molecular photoinduced energy- and electron-transfer processes have been investigated in systems in which MP−C_{60} and *n*TV ($n = 2$−4) are covalently linked (Chart 2). The results indicate that, in ODCB, an *intra*molecularly charge-separated state is formed in a two-step mechanism involving a fast singlet energy transfer followed by electron transfer. In toluene, the experimental observations are consistent with the presence of two competing processes after photoexcitation of the *n*TV moiety and subsequent singlet energy transfer from the *n*TV-(S_1) to the MP−C_{60}(S_1) state: (a) electron transfer leading to an *intra*molecularly charge-separated state ($C_{60}^{-\bullet}$− *n*TV$^{+\bullet}$ for C_{60}−3TV and C_{60}−4TV−C_{60}) in which the charges recombine rapidly, bringing the two moieties back to their ground states, and (b) fluorescence and intersystem crossing to MP−C_{60}(T_1) (for C_{60}−2TV and C_{60}−3TV), followed by triplet energy transfer to *n*TV(T_1) in the case of C_{60}−3TV. The relative extents of the two competing processes depend on the relative energetic positions of the MP−C_{60}(S_1) and the *intra*molecularly charge-separated states, which can be controlled by the polarity of the solvent. In toluene, process a does not occur for C_{60}−2TV, whereas b is essentially absent for C_{60}−4TV−C_{60}.

The distinction between photoinduced energy- and electron-transfer processes (both *inter*- and *intra*molecular) was semiquantitatively analyzed with the Weller equation (eq 6).

Future experiments using femtosecond pump−probe spectroscopy on longer *n*TV−C_{60} dyads and triads[44] will be performed to investigate the competition between thermal decay and energy and electron transfer on short time scales in order to assess the potential of thienylenevinylenes for photovoltaic energy conversion in more detail.

4. Experimental Section

The synthesis of the thienylenevinylene oligomers has been described in detail previously.[21,43] The syntheses of the covalently linked dyads and triad were performed using *N*-methylglycine, [60]fullerene, and the corresponding oligothienylenevinylene mono- or dialdehyde.[45] As the formation of the pyrolidine ring creates a stereocenter, C_{60}−2TV and C_{60}−3TV are mixtures of two stereoisomers, and C_{60}−4TV−C_{60} is a mixture of two diasteroisomers. Full details of the synthesis and characterization will be described elsewhere.[44] UV/vis absorption spectra were recorded on a Perkin-Elmer Lambda 900 or Lambda 40P spectrophotometer. Low-temperature spectra were recorded using an Oxford Optistat continuous-flow cryostat; during measurements, the temperature was kept constant to within 0.5 K. Spectra at different temperatures were not corrected for volume changes of the solvents. Fluorescence spectra were recorded on a Perkin-Elmer LS 50B spectrometer or an Edinburgh Instruments FS920 double-monochromator spectrometer using a Peltier-cooled red-sensitive photomultiplier. Fluorescence quantum yields were determined using anthracene (in ethanol) and quininesulfatedihydrate (in 1 N H_2SO_4) as a reference.[46] Time-correlated single-photon-counting photoluminescence studies were performed using an Edinburgh Instruments LifeSpec-PS system consisting of a 400-nm picosecond laser operated at 2.5 MHz and a Peltier-cooled Hamamatsu microchannel plate photomultiplier (R3809U-50). Lifetimes were determined using the Edinburgh Instruments software

package. For all PL studies, the optical densities of the solutions were adjusted to 0.1 at the excitation wavelength.

Photoinduced absorption (PIA) spectra were recorded between 0.25 and 3 eV by exciting the sample contained in a sealed 1-mm near-IR-grade quartz cell with a mechanically modulated (typically 275 Hz) cw Ar-ion laser (Spectra Physics 2025) pump beam (25 mW, beam diameter of 2 mm) and monitoring the resulting change in transmission (ΔT) of a tungsten−halogen white-light probe beam after dispersion by a triple grating monochromator, using Si, InGaAs, and (cooled) InSb detectors. The PIA spectra were recorded with the pump beam in an almost parallel direction to the probe beam. Oxygen-free solutions were studied at room temperature. Excited-state lifetimes were determined by fitting the change in transmission as a function of the modulation frequency (ω) to the expression for either monomolecular decay (eq 4) or for bimolecular decay (eq 5).

Acknowledgment. This research was supported by The Netherlands Organization for Chemical Research (CW), The Netherlands Organization for Scientific Research (NWO), through a grant in the PIONIER program. Stefan Meskers is acknowledged for discussions.

References and Notes

(1) Sariciftci, N. S.; Heeger, A. J. *Int. J. Mod. Phys. B* **1994**, *8*, 237.

(2) Yu, G.; Gao, J.; Hummelen, J. C.; Wudl, F.; Heeger, A. J. *Science* **1995**, *270*, 1789.

(3) Brabec, C. J.; Padinger, F.; Hummelen, J. C.; Janssen, R. A. J.; Sariciftci, N. S. *Synth. Met.* **1999**, *102*, 861.

(4) Shaheen, S. E.; Brabec, C. J.; Sariciftci, N. S.; Padinger, F.; Fromerz, T.; Hummelen, J. C. *Appl. Phys. Lett.* **2001**, *78*, 841.

(5) Roman, L. S.; Andersson, M. R.; Yohannes, T.; Inganäs, O. *Adv. Mater.* **1997**, *9*, 1164.

(6) Ouali, L.; Krasnikov, V. V.; Stalmach, U.; Hadziioannnou, G. *Adv. Mater.* **1999**, *11*, 1515.

(7) Sariciftci, N. S.; Smilowitz, L.; Heeger, A. J.; Wudl, F. *Science* **1992**, *258*, 1474.

(8) (a) Kraabel, B.; McBranch, D.; Sariciftci, N. S.; Moses, D.; Heeger, A. J. *Phys. Rev. B* **1994**, *50*, 18543. (b) Kraabel, B.; Hummelen, J. C.; Vacar, D.; Moses, D.; Sariciftci, N. S.; Heeger, A. J.; Wudl, F. *Phys. Rev. B* **1994**, *50*, 18543. (c) Moses, D.; Dogariu, A.; Heeger, A. *J. Chem. Phys. Lett.* **2000**, *316*, 356.

(9) Brabec, C. J.; Zerza, G.; Cerullo, G.; De Silvestri, S.; Luzatti, S.; Hummelen, J. C.; Sariciftci, N. S. *Chem. Phys. Lett.* **2001,** *340*, 232.

(10) Meskers, S. C. J.; van Hal, P. A.; Spiering, A. J. H.; van der Meer, A. F. G.; Hummelen, J. C.; Janssen, R. A. J. *Phys. Rev. B.* **2000**, *61*, 9917.

(11) Segura, J. L.; Gómez, R.; Martín, N.; Luo, C.; Guldi, D. M. *Chem. Commun.* **2000**, 701.

(12) Martini, I. B.; Ma, B.; Da Ros, T.; Helgeson, R.; Wudl, F.; Schwartz, B. *J. Chem. Phys. Lett.* **2000**, *327*, 253.

(13) van Hal, P. A.; Knol, J.; Langeveld-Voss, B. M. W.; Meskers, S. C. J.; Hummelen, J. C.; Janssen, R. A. J. *J. Phys. Chem. A* **2000**, *104*, 5974.

(14) Peeters, E.; van Hal, P. A.; Knol, J.; Brabec, C. J.; Sariciftci, N. S.; Hummelen, J. C.; Janssen, R. A. J. *J. Phys. Chem. B* **2000**, *104*, 10174.

(15) (a) van Hal, P. A.; Janssen, R. A. J.; Lanzani, G.; Cerullo, G.; Zavelani-Rossi, M.; De Silvestri, S. *Phys. Rev. B* **2001**, *64*, 075206. (b) van Hal, P. A.; Janssen, R. A. J.; Lanzani, G.; Cerullo, G.; Zavelani-Rossi, M.; De Silvestri, S. *Chem. Phys. Lett.* **2001**, *345*, 33.

(16) Knorr, S.; Grupp, A.; Mehring, M.; Grube, G.; Effenberger, F. *J. Chem. Phys.* **1999**, *110*, 3502.

(17) Yamashiro, T.; Aso, Y.; Otsubo, T.; Tang, H.; Harima, Y.; Yamashita, K. *Chem. Lett.* **1999**, 443.

(18) Armaroli, N.; Barigelletti, F.; Ceroni, P.; Eckert, J. F.; Nicoud, J. F.; Nierengarten, J. F. *Chem. Commun.* **2000**, 599.

(19) Eckert, J. F.; Nicoud, J. F.; Nierengarten, J. F.; Liu, S. G.; Echegoyen, L.; Barigelletti, F.; Armaroli, N.; Ouali, L.; Krasnikov, V. V.; Hadziioannnou, G. *J. Am. Chem. Soc.* **2000**, *122*, 7467.

(20) Fujitsuka, M.; Ito, O.; Yamashiro, T.; Aso, Y.; Otsubo, Y. *J. Phys. Chem. A* **2000**, *104*, 4876.

(21) (a) Roncali, J. *Acc. Chem. Res*. **2000**, *33*, 147. (b) Jestin, I.; Frère, P.; Blanchard, P.; Roncali, J. *Angew. Chem., Int. Ed. Engl.* **1998**, *37*, 942. (c) Jestin, I.; Frère, P.; Mercier, N.; Levillain, E.; Stievenard, D.; Roncali, J. *J. Am. Chem. Soc.* **1998**, *120*, 8150.

(22) (a) Bäuerle, P.; Fisher, T.; Bidlingmeier, B.; Stabel, A.; Rabe, J. P. *Angew. Chem., Int. Ed. Engl.* **1995**, *34*, 303. (b) Meier, H.; Stalmach, U.; Kolshorn, H. *Acta Polym.* **1999**, *48*, 379. (c) van Haare, J. A. E. H.; Havinga, E. E.; van Dongen, J. L. J.; Janssen, R. A. J.; Cornil, J.; Brédas, J.-L. *Chem. Eur. J.* **1998**, *4*, 1509. (d) Peeters, E.; Marcos, A.; Meskers, S. C. J.; Janssen, R. A. J. *J. Chem. Phys.* **2000**, *112*, 9445.

(23) Krzeminski, C.; Delerue, C.; Allan, G.; Haguet, V.; Stievenard, D.; Frère, P.; Levillain, E.; Roncali, J. *J. Chem. Phys.* **1999**, *111*, 6643.

(24) (a) Hirsch, A. *The Chemistry of the Fullerenes*; Thieme: Stuttgart, Germany, 1994. (b) Prato, M. *J. Mater. Chem.* **1997**, *7*, 1097. (c) *Fullerenes and Related Structures, Topics in Current Chemistry*; Hirsch, A., Ed.; Springer-Verlag: Berlin/Heidelberg, 1999.

(25) (a) Imahori, H.; Sakata, Y. *Adv. Mater.* **1997**, *9*, 537. (b) Martin, N.; Sánchez, L.; Illescas, B.; Pérez, I. *Chem. Rev.* **1998**, *98*, 2527. (c) Imahori, H.; Sakata, Y. *Eur. J. Org. Chem.* **1999**, 2445.

(26) Gust, D.; Moore, T. A.; Moore, A. L. *Acc. Chem. Res.* **2001**, *34*, 40.

(27) Luo, C.; Guldi, D. M.; Imahori, H.; Tamaki, K.; Sakata, Y. *J. Am. Chem. Soc.* **2000**, *122*, 6535.

(28) Armaroli, N.; Marconi, G.; Echegoyen, E.; Bourgeois, J. P.; Diederich, J. F. *Chem. Eur. J.* **2000**, *6*, 1629.

(29) (a) Brassett, A. J.; Colaneri, N. F.; Bradley, D. D. C.; Lawrence, R. A.; Friend, R. H.; Murata, H.; Tokito, S.; Tsutsui, T.; Saito, S. *Phys. Rev. B* **1990**, *41*, 10586. (b) Samuel, I. D. W.; Meyer, K. E.; Bradley, D. D. C.; Friend, R. H. *Synth. Met.* **1991**, *41*, 1377. (c) Frolov, S.; Leng, J. M.; Vardeny, Z. V. *Mol. Cryst. Liq. Cryst.* **1994**, *256*, 473. (d) Lies, M.; Jeglinski, S.; Lane, P. A.; Vardeny, Z. V. *Synth. Met.* **1997**, *84*, 891.

(30) Turro, N. J. *Modern Molecular Photochemistry*; University Science Books: Mill Valley, CA, 1991.

(31) Strickler, S. J.; Berg, R. A. *J. Chem. Phys*. **1962**, *37*, 814.

(32) Kohler, B. E. In *Conjugated Polymers: The Novel Science and Technology of Highly Conducting and Nonlinear Optically Active Materials*; Brédas, J. L., Silbey, R. J., Eds.; Kluwer Academic Publishers: Dordrecht, The Netherlands, 1991; pp 405−434.

(33) (a) Kobayashi, T.; Yasuda, M.; Okada, S.; Matsuda, H.; Nakanishi, H. *Chem. Phys. Lett.* **1997**, *267*, 472. (b) Lawrence, B.; Torruellas, W. E.; Cha, M.; Sundheimer, M. L.; Stegeman, G. I.; Meth, J.; Etemad, S.; Baker, G. *Phys. Rev. Lett.* **1994**, *73*, 597.

(34) Williams, R. M.; Zwier, J. M.; Verhoeven, J. W. *J. Am. Chem. Soc.* **1995**, *117*, 4093.

(35) The lifetime of the MP−C_{60} state as determined in oxygen-free solutions with the modulated cw-PIA technique using eq 4 provides a lifetime of 240 μs (see also refs 13 and 14). Using other experimental techniques, triplet lifetimes for related C_{60} derivatives have been published that are almost 1 order of magnitude less. See refs 6, 27, and (a) Liddell, P. A.; Kuciauskas, D.; Sumida, J. P.; Nash, B.; Nguyen, D.; Moore, A. L.; Moore, T. A.; Gust, D. *J. Am. Chem. Soc.* **1997**, *119*, 1400. (b) Anderson, J. L.; An, Y. Z.; Rubin, Y.; Foote, C. S. *J. Am. Chem. Soc.* **1994**, *116*, 9763.

(36) (a) Thomas, K. G.; Biju, V.; George, M. V.; Guldi, D. M.; Kamat, P. V. *J. Phys. Chem. A* **1998**, *102*, 7580. (b) Guldi, D. M.; Maggini, M.; Scorrano, G.; Prato, M. *J. Am. Chem. Soc.* **1997**, *119*, 974.

(37) Apperloo, J. J.; Raimundo, J.-M.; Frère, P.; Roncali, J.; Janssen, R. A. J. *Chem. Eur. J.* **2000**, *6*, 1698.

(38) Dellepiane, G.; Cuniberti, C.; Comoretto, D.; Musso, G. F.; Figari, G.; Piaggi, A.; Borghesi, A. *Phys. Rev. B.* **1993**, *48*, 7850.

(39) The toluene solutions containing MP−C_{60} and *n*TV were stable against 25-mW laser excitation, whereas, in ODCB, some decomposition (up to ∼10%) clearly occurs during the PIA measurements.

(40) Weller, A. *Z. Phys. Chem. Neue Folge* **1982**, *133*, 93.

(41) Williams, R. M.; Koeberg, M.; Lawson, J. M.; An, Y. Z.; Rubin, Y.; Paddon-Row, M. N.; Verhoeven, J. W. *J. Org. Chem.* **1996**, *61*, 5055.

(42) Beljonne, D.; Cornil, J.; Friend, R. H.; Janssen, R. A. J.; Brédas, J.-L. *J. Am. Chem. Soc.* **1996**, *118*, 6453.

(43) (a) Elandaloussi, E.; Frère, P.; Roncali, J. *Chem. Commun.* **1997**, 301. (b) Elandaloussi, E.; Frère, P.; Richomme, P.; Orduna, J.; Garin, J.; Roncali, J. *J. Am. Chem. Soc.* **1997**, *121*, 88760.

(44) Martineau, C.; Roncali, J., manuscript to be published.

(45) Maggini, M.; Scorrano, G.; Prato, M. *J. Am. Chem. Soc.* **199**3, *11*5, 9798.

(46) Eaton, D. F. *Pure Appl. Chem*. **1988**, *60*, 1107.